

Physical conditions in metal line systems toward Q 1037-2704: Evidence for superclustering at $z \sim 2^*$ **

Yannick Lespine¹ and Patrick Petitjean^{1,2}

¹Institut d'Astrophysique de Paris - CNRS, 98bis Boulevard Arago, F-75014 Paris, France

²UA CNRS 173 - DAEC, Observatoire de Paris-Meudon, F-92195 Meudon Principal Cedex, France

Abstract. We present a high spectral resolution optical spectrum (FWHM = 17 km s⁻¹) of the bright quasar Q 1037-2704. The large number of absorption systems suggests the presence of an intervening supercluster, but the issue remains controversial.

We demonstrate that the strong C IV system at $z_{\text{abs}} \sim 2.08$ spanning more than 1500 km s⁻¹ is made up of narrow components with typical Doppler parameter $b \sim 8$ km s⁻¹. The gas is probably photo-ionized in which case the photo-ionizing spectrum should be dominated by stellar radiation. Analysis of H I, Si IV, N V and C IV absorptions shows that the gas has a fairly large metal content, $Z > 0.1 Z_{\odot}$.

We detect C II* λ 1335 absorption in subcomponents of the $z_{\text{abs}} \sim 2.133$ system, which have moderate total C II column densities implying an electronic density of $n_e \sim 3$ cm⁻³. In addition, the weakness of the O I λ 1302, Si II λ 1304 and Fe II λ 1608 lines allows a detailed analysis of the line profiles. The results are that the system has four narrow ($b \sim 10$ km s⁻¹) components; the oxygen abundance is of the order of 0.03 solar; the iron abundance is surprisingly large [Fe/O] \sim [Fe/O]_⊙ + 0.3. If photo-ionized by the UV flux from the quasar, the distance between the absorber and the quasar should be larger than $0.3h^{-1}$ Mpc (with h in units of $H_0 = 100$ km s⁻¹ Mpc⁻¹ and $q_0 = 0.5$).

This demonstrates that the gas is not associated with the quasar and, together with the detection of eight multiple metal systems between $z_{\text{abs}} = 1.91$ and 2.13, suggests the presence of a coherent structure extended over $80h^{-1}$ Mpc along the line of sight.

Key words: intergalactic medium, quasars: absorption lines

1. Introduction

Evolution of large scale structures of the Universe is one of the most important issues of modern cosmology. QSO absorption line systems probe material lying on the line of sight to quasars over a large redshift range ($0 < z < 5$), and can thus be used as luminosity unbiased tracers of these structures over most of the history of the Universe.

This has been recognized for over a decade (e.g. Shaver & Robertson 1983, Robertson & Shaver 1983). Observations of QSO pairs with projected separations from a few arcseconds to a few arcminutes yield interesting constraints on the size, physical structure and kinematics of galactic haloes, clusters and filaments. Indeed, new constraints have been obtained very recently on the extent of the Ly α complexes perpendicular to the line of sight at high (Smette et al. 1992, 1995, Bechtold et al. 1994, Dinshaw et al. 1994) and intermediate (Dinshaw et al. 1995) redshifts indicating that they could have sizes larger than 300 kpc. Such sizes are more indicative of a correlation length than of real cloud sizes (Rauch & Haenelt 1996). This is consistent with the picture that the Ly α gas traces the potential wells of dark matter filamentary structures (Cen et al. 1994, Petitjean et al. 1995, Mückel et al. 1996, Hernquist et al. 1996). Large scale clustering of C IV systems (Heisler et al. 1989; Foltz et al. 1993) or damped systems (Francis & Hewett 1993, Wolfe 1993) have also been detected recently. The advent of 10m-class telescopes will boost this field since faint QSOs in the same field will allow 3-D mapping of the baryonic content of the universe via absorption line systems (Petitjean 1995).

It is well known that formation of structures by gravitational instability depends sensitively on the value of Ω and on the primordial density fluctuation spectrum. In particular, observation of substructures in present day clusters (West 1994) may indicate that the clusters have not finished evolving at $z \sim 0$, and favor high density universes ($\Omega > 0.5$, Richstone et al. 1992, Jing et al. 1995) in contradiction with other determinations ($\Omega \sim 0.2-0.3$, e.g. Ostriker 1993). Therefore, the search for high redshift clusters may yield important clues on how structures form and subsequently merge, and so may be used to constrain cosmological parameters (e.g. Evrard & Charlot 1994).

In this context, the field surrounding the bright ($m_V = 17.4$) high redshift ($z_{\text{em}} = 2.193$) QSO Tol Q1037-2704 is quite promising. Jakobsen et al. (1986) were the first to note

Send offprint requests to: P. Petitjean

*Based on observations collected at the European Southern Observatory, La Silla, Chile.

**Table 1 only available in electronic form at the CDS via anonymous ftp to cdsarc.u-strasbg.fr (130.79.128.5) or via <http://cdsweb.u-strasbg.fr/Abstract.html>

the remarkable similarity of the metal-line absorption systems in the spectra of Tol 1037-2704 and Tol 1038-2712 separated by 17.9 on the sky, corresponding to $4.3h_{100}^{-1}$ Mpc for $q_o = 0.5$ at $z \sim 2$. They interpreted this as evidence for the presence of a supercluster along the line of sight to the QSOs. The fact that the number of metal-line systems in both spectra over the range $1.90 \leq z \leq 2.15$ is far in excess of what is usually observed has been considered as the strongest argument supporting this conclusion (Ulrich & Perryman 1986, Sargent & Steidel 1987, Robertson 1987). In a recent paper, Dinshaw & Impey (1996, hereafter DI96) have presented new data on four quasars in this field. They find that the velocity correlation function of the C IV systems shows strong and significant clustering for velocity separations less than 1000 km s⁻¹ and up to 7000 km s⁻¹ respectively. The spatial correlation function shows a marginally significant signal on scales of < 18 Mpc. They conclude that the dimensions of the proposed supercluster are at least $30 h^{-1}$ Mpc on the plane of the sky and approximately $80 h^{-1}$ Mpc along the line of sight.

It is however not excluded that at least some of the systems, in particular those spanning more than 1000 km s⁻¹ at $z_{\text{abs}} \sim 2.08$ and $z_{\text{abs}} \sim 2.13$, originate in gas ejected from the quasars. The fact that they are common to both Tol 1037-2704 and Tol 1038-2712 lines of sight could be due to chance coincidence (Cristiani et al. 1987).

The importance of clarifying the presence of such a large structure at $z \sim 2$ led us to observe Tol 1037-2704 at a spectral resolution twice as high as previous observations, in order to be able to discuss the physical state of the gas in the $z_{\text{abs}} \sim 2.08$ and $z_{\text{abs}} \sim 2.13$ systems. New optical data are presented in Section 2 and discussed in Section 3. We draw our conclusions in Section 4.

2. The data

2.1. Observations

The observations were carried out at the F/8 Cassegrain focus of the 3.6 m telescope at La Silla, ESO Chile. The spectra were obtained with the ESO echelle spectrograph (CASPEC) during two observing runs: three exposures of 5400 s each were obtained under good seeing conditions in December 1992; two additional 5400 s exposures were taken in April 1994 during cloudy nights. A 300 line mm⁻¹ cross disperser was used in combination with a 31.6 line mm⁻¹ echelle grating. The detector was a Tektronix CCD with 568×512 pixels of 27 μm square and a read-out noise of 10 electrons. For each exposure on the object flat field images and wavelength comparison Thorium–Argon spectra were recorded. The slit width was 2" corresponding to a spectral resolution of $R \sim 18000$. The accuracy in the wavelength calibration measured on the calibrated Thorium–Argon spectra is about 0.03 Å.

The data were reduced using the echelle reduction packages provided by IRAF and MIDAS. The cosmic-ray events have been removed in the regions between object spectra before extraction of the object. Several exposures were co-added to increase the signal to noise ratio. During this merging procedure the cosmic-ray events affecting the object pixels were recognized and eliminated, a procedure that worked well since five exposures were available. The background sky spectrum was difficult to extract separately due to the small spacing between the orders in the blue. Instead, we have carefully fitted the zero level to the bottom of the numerous saturated lines

in the Lyα forest. The uncertainty on the determination can be estimated to be 5%. The normalized spectrum is shown in Fig. 1.

We identify all the absorption features with equivalent widths larger than $5 \times \text{FWHM} \times \sigma$ where σ is the noise rms in the adjacent continuum and use the linelist to recognize the systems. A system is identified when the wavelength agreement between two lines of a doublet found beyond the Lyα forest is better than 0.1 Å and when the strengths of the two lines are consistent with the corresponding oscillator strength ratio. All the systems listed in Section 2.2 have doublets redshifted beyond the Lyα forest. The whole spectrum is then searched for additional lines. For isolated lines, the same criterion on the wavelength is used. For strong blends, the identification is based on the consistency of the line profiles (see e.g. Fig. 2). All features detected in the spectrum are described in Table 1 and identification is given when possible. We then have fitted Voigt profiles convolved with the instrumental profile to all the identified absorption lines using the package FIT/LYMAN recently implemented in MIDAS. The atomic data are taken from Morton et al. (1988), Morton (1991) and Tripp et al. (1996). The systems are considered made up of components. For each of the latter the redshift, temperature, and turbulent Doppler parameter are assumed the same for the high-ionization (C IV, Si IV) and low-ionization (C II, O I, Al II, Si II, Fe II) species. The model is fitted to all the absorption lines of the system at the same time minimizing the χ^2 and the number of subcomponents. In the case large Doppler parameters are found, especially in the centre of strong blends, it is probable that several subcomponents are present. As shown by Jenkins (1986), the Doppler parameter is then indicative of the number of subcomponents and, if the lines are not strongly saturated, the column density is a good estimate of the sum of the column densities in all subcomponents. The case of the $z_{\text{abs}} = 2.081$ system is peculiar as tight constraints on the Doppler parameter can be placed because some of the lines are saturated but do not go to the zero level. In this system we find $b \lesssim 8$ km s⁻¹. The vacuum heliocentric redshifts, velocity dispersions and column densities of subcomponents are given in Table 1. The typical error on the column densities is 0.15 in units of log N except for heavily blended lines marked in the Table.

2.2. Comments on individual systems

2.2.1. Galactic absorption

We detect a galactic Ca II λ3934,3969 doublet with equivalent widths 0.48, 0.30 Å and heliocentric velocity $v = 3.3$ km s⁻¹. The column density and Doppler parameter are $10^{13.2}$ cm⁻² and 12.6 km s⁻¹.

2.2.2. $z_{\text{abs}} = 0.6964$

This Mg II system, detected at the 5σ level, shows two resolved components separated by about 35 km s⁻¹. Fe II λ2382 is not detected and should have $w_r < 0.11$ Å. It is interesting to note that Jakobsen & Perryman (1992) detect a strong Mg II system at $z_{\text{abs}} = 0.643$ in BW15 (see Bohuski & Weedman 1979). The 3D distance between the two systems is about $200h_{100}^{-1}$ Mpc at $z = 0.696$.

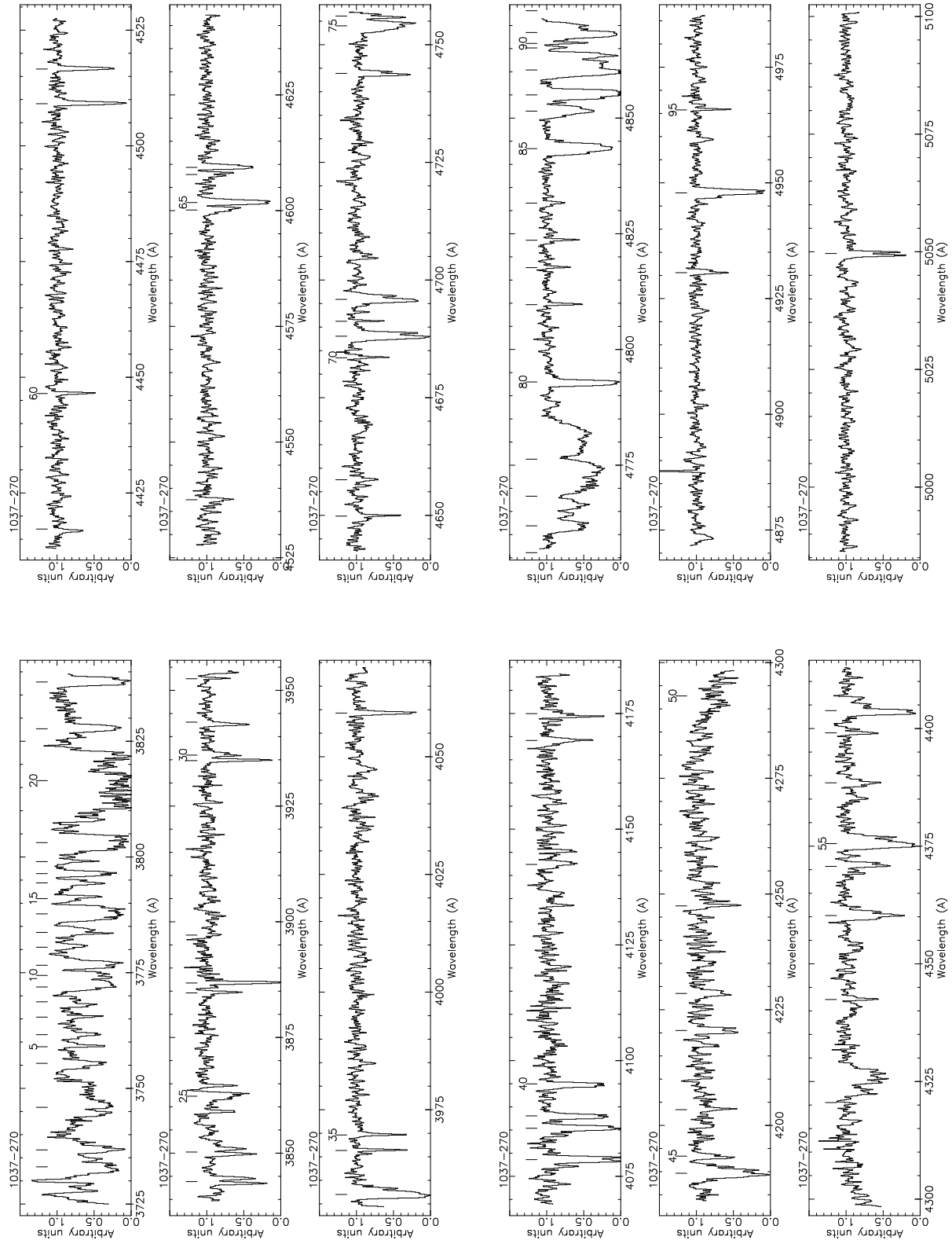


Fig. 1. Normalized spectrum of Tol 1037-270

2.2.3. $z_{\text{abs}} = 1.0765$

We detect Fe II $\lambda\lambda 2344, 2374, 2382$ lines in this Mg II system (Jakobsen et al. 1986). At our resolution, the line profiles indicate the presence of three components spread over 72 km s^{-1} .

2.2.4. $z_{\text{abs}} = 1.4829$

The redshift coincidence of the two C IV lines in this system is very good. There are two detached components with velocity separation $\Delta V \sim 97 \text{ km s}^{-1}$. The corresponding Al III lines have $w_r < 0.04 \text{ \AA}$.

2.2.5. $z_{\text{abs}} = 1.6345$

This system has two strong components separated by 50 km s^{-1} and an additional detached satellite displaced 100 km s^{-1} to the blue. The corresponding Al III lines have $w_r < 0.05 \text{ \AA}$. Considering the lines as optically thin, this corresponds to $N(\text{Al III}) < 3 \times 10^{12} \text{ cm}^{-2}$. Given the C IV column density derived from line profile fitting (see Table 1), we obtain $N(\text{C IV})/N(\text{Al III}) > 86$. This is four times larger than the maximum of this ratio observed in the Galactic halo (Sembach & Savage 1992).

2.2.6. $z_{\text{abs}} = 1.9125$

This is a strong system with very good wavelength coincidences. Si IV $\lambda 1402$ is blended with C IV $\lambda 1550$ at $z_{\text{abs}} = 1.6345$. We detect strong absorptions by C II $\lambda 1334$, Si II $\lambda 1526$ and Al II $\lambda 1670$. The fit with one component is very good. However the strength of C II $\lambda 1334$ suggests the presence of subcomponents.

Using Bergeron & Stasińska (1986) and Petitjean et al. (1994) models, we can estimate the characteristics of the gas. From $\log N(\text{Si II})/N(\text{Si IV}) \sim 0.1$ and $\log N(\text{C II})/N(\text{C IV}) \sim 0.6$, we derive an ionization parameter U close to 2×10^{-3} . Using $w_r \sim 0.9 \text{ \AA}$ for the H I Ly α line (Sargent & Steidel 1987) we find 10^{17} cm^{-2} for $b < 40 \text{ km s}^{-1}$. From this we can conclude that all the column densities are indicating abundances close to but smaller than $0.1 Z_{\odot}$. Note that the Al II column density is consistent with this conclusion. This is an indication that the system is not associated with the quasar (Petitjean et al. 1994).

2.2.7. $z_{\text{abs}} = 1.9722$

This strong C IV system is a blend of four components spread over 130 km s^{-1} ; three of them have an associated Si IV absorption. The strongest component has narrow ($b < 10 \text{ km s}^{-1}$) and well defined C II, Si II and Al II absorption lines. The column density ratios (see Table 1) are similar to that obtained for the $z_{\text{abs}} = 1.9125$ system. The H I column density should be larger than 10^{18} cm^{-2} , from the Ly α line equivalent width (Sargent & Steidel 1987). The abundances are therefore most certainly smaller than $0.1 Z_{\odot}$ as in the $z_{\text{abs}} = 1.9125$ system.

2.2.8. $z_{\text{abs}} = 2.0034$

This is a weak ($w_r(1548,1550) = 0.27, 0.15 \text{ \AA}$) C IV system. No other line is detected.

2.2.9. $z_{\text{abs}} = 2.0280$

Two strong components separated by 50 km s^{-1} and a weak satellite 275 km s^{-1} to the blue are seen in this system. The weak detached lines have $b < 10 \text{ km s}^{-1}$ consistent with photo-ionization. C II $\lambda 1334$ is at our detection limit (see DI96). We do not detect the component at $z_{\text{abs}} = 2.03915$ (DI96).

2.2.10. $z_{\text{abs}} \sim 2.081$

This redshift is common to both Tol 1037-2704 and Tol 1038-2712 lines of sight (DI96). The system shows absorption spread over the redshift range $2.0699 < z < 2.0879$ or 1750 km s^{-1} . The C IV lines are weakly saturated (the equivalent widths ratio is different from the oscillator strength ratio) but do not go to the zero level (see Section 3.1). The Ly α and Si IV lines (at 3748 and 4294 \AA respectively) are weak. We cannot exclude weak N V absorption since strong H I and Si III lines at $z_{\text{abs}} = 2.133$ are present in the redshifted N V wavelength range. Even at our resolution the C IV profile does not break into components suggesting absorption by a continuous medium. The appearance of such complex may lead Tol 1037-2704 to be classified as a BAL QSO (Weymann et al. 1981). This is the reason why a detailed discussion of the physical state of the absorbing gas is useful (see Section 3.1).

2.2.11. $z_{\text{abs}} = 2.1067$ and 2.1157

These are weak ($w_r(1548,1550) = 0.07, 0.04 \text{ \AA}$ and $0.06, 0.04 \text{ \AA}$) C IV systems with a single narrow ($b \sim 10 \text{ km s}^{-1}$) component. No other line is detected.

2.2.12. $z_{\text{abs}} \sim 2.133$

The C IV absorption is spread over the redshift range $2.1279 < z < 2.1403$ or 1190 km s^{-1} . It shows well detached saturated complexes. The line profile is complex but not as smooth as the $z_{\text{abs}} = 2.081$ profile. Visually there are two well defined components at $z_{\text{abs}} = 2.1392$ and 2.1396 seen in O I $\lambda 1302$, Si II $\lambda 1304$, Fe II $\lambda 1608$ and C II* $\lambda 1335$ (see Section 3.2). DI96 identified the $\lambda 4193.4$ feature as C II $\lambda 1334$ at $z_{\text{abs}} = 2.14233$ on the basis of the presence of C IV $\lambda\lambda 1548, 1550$ and Si IV $\lambda 1393$ at the same redshift. However, in the DI96 data, some of these features are blended with other lines. At our higher spectral resolution, we find that, if the C II $\lambda 1334$ identification is correct, the redshift disagreement with C IV is about 30 km s^{-1} that is larger than our resolution. Moreover, at this redshift, we see neither Si IV $\lambda 1393$ nor Si II $\lambda 1260$ which is as strong as C II $\lambda 1334$ in neighbouring components. On the contrary, the identification as C II* $\lambda 1335$ gives nearly perfect redshift agreement with O I, Si II and Fe II (see Fig. 2). We therefore believe that the identification as C II* $\lambda 1335$ is secure. This makes the detailed studying of this system of great importance for discussing the origin of the gas (see Section 3.2).

It is interesting to note that a narrow and single N V $\lambda 1238$ line is detected at $z_{\text{abs}} = 2.1358$. N V $\lambda 1242$ is at our detection limit.

3. Physical state of the gas

To ascertain the possible presence of a large concentration of gas possibly extended over $30h^{-1} \text{ Mpc}$ perpendicular to the line of sight and $80h^{-1} \text{ Mpc}$ along the line of sight (DI96), we use our data to make a detailed analysis of the $z_{\text{abs}} = 2.081$

Table 1. Absorption lines

λ_{helio} (Å)	w_{obs} (Å)	σ_w^a	Identification	z_{abs}	n	$\log N$ (cm^{-2})	b (km s^{-1})	z_c	
1037-270									
1	3733.05	2.17	0.04	HI λ 1215	2.0707	1	13.5 ^b	45.0	2.06978
						2	13.5 ^b	22.0	2.07008
						3	13.5 ^b	22.0	2.07031
						4	13.5 ^b	45.0	2.07060
						5	13.5 ^b	38.0	2.07097
						6	13.5 ^b	48.0	2.07124
2	3736.70	1.45	0.04						
3	3745.90	5.60	0.04	HI λ 1215	2.0800				
				SiII λ 1260	1.9721				
				SiIII λ 1206	2.1066				
4	3755.40	1.14	0.04						
5	3758.99	0.63	0.04	SiIII λ 1206	2.1156	13.12	28.3	2.11562	
1037-270 Continued									
27	3886.77	0.61	0.04	CII λ 1334	1.9125		14.8 ^b	15.0	1.91246
28	3897.12	0.04	0.03	NV λ 1242	2.1357				
29	3934.82	0.48	0.02	CaII λ 3934	0.0000		13.02	12.6	0.00001
30	3936.00	0.33	0.02						
31	3943.13	0.42	0.02	SiII λ 1260	2.1284		12.91	14.1	2.12788
32	3952.50	0.09	0.02						
33	3957.00	1.90	0.03	SiII λ 1260	2.1394	1	14.00	12.3	2.13892
						2	14.03	11.3	2.13913
						3	14.17	12.8	2.13938
						4	13.74	13.7	2.13955
						5	13.09	14.0	2.13986
						6	12.92	13.6	2.14037

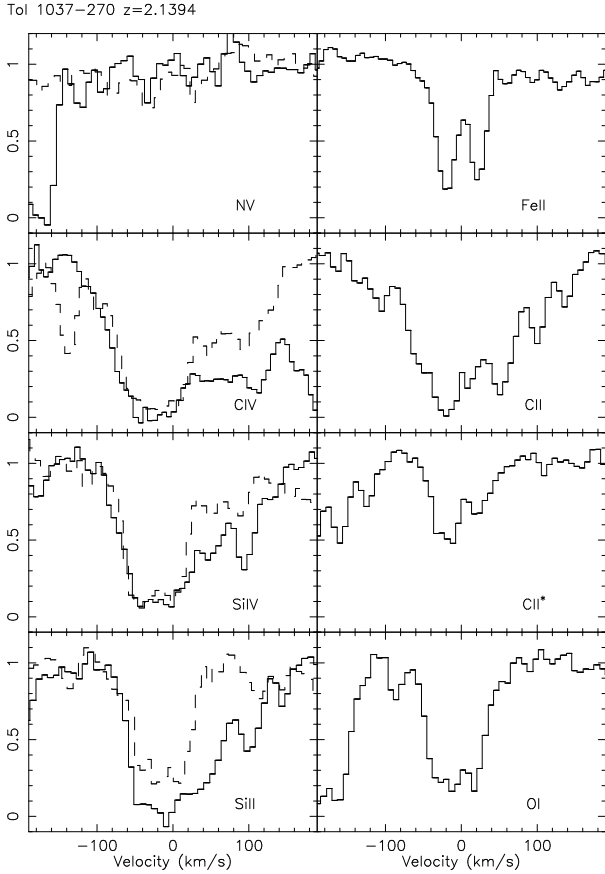


Fig. 2. Absorption lines in the $z_{\text{abs}} \sim 2.133$ system on a relative velocity scale. The redshift for zero velocity is given at the top. When several lines of the same ion are present in the data the corresponding parts of the spectrum are overplotted, with solid, dashed and dotted lines in order of decreasing oscillator strengths. CII is for CII λ 1334, CII* for CII λ 1335, CIV for CIV λ 1548,1550, OI for OI λ 1302, SiII for SiII λ 1260,1304, SiIV for SiIV λ 1393,1402, FeII for FeII λ 1608

and 2.133 systems to differentiate between the ejection and the intervening hypotheses for the origin of these systems.

3.1. The $z_{\text{abs}} \sim 2.081$ system

It can be seen in Fig. 3 that the C IV lines do not go to the zero level. Most of the components have apparent optical depth smaller than 0.7. It is therefore expected that the apparent optical depth ratio $\tau(\lambda 1548)/\tau(\lambda 1550)$ is approximately equal to the oscillator strength ratio, $f(\lambda 1548)/f(\lambda 1550) = 2$, if the lines are resolved. It is apparent that this is not true: $\tau(\lambda 1548)/\tau(\lambda 1550) < 1.5$. This suggests either that the absorbing cloud do not cover the continuum or that the cloud is made up of unresolved components. Several arguments favor the later assumption. The velocity difference between the absorber and the quasar ($z_{\text{em}} = 2.193$, Sargent & Steidel 1987) is about 10000 km s^{-1} , with no trace of similar absorption at smaller velocity difference (see Section 3.2 for discussion of the $z_{\text{abs}} \sim 2.133$ system). In order to partially cover the continuum source, the clouds must be small and close to the quasar. However, the system is common to Tol 1037-2704 and Tol 1038-

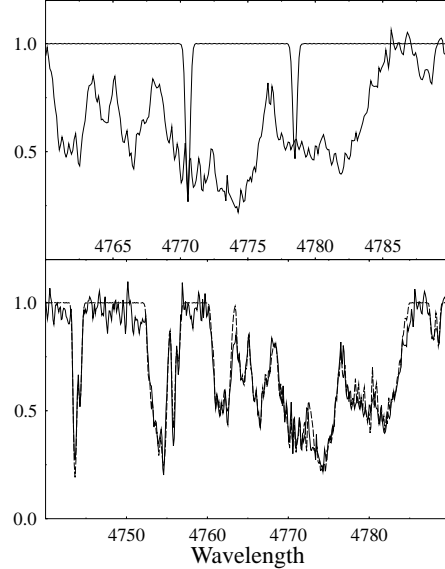


Fig. 4. Fit to the C IV absorption at $z_{\text{abs}} = 2.081$. In the upper panel a one component C IV doublet with $b = 7 \text{ km s}^{-1}$ and $\log N = 13.65$ is overplotted on the spectrum. This illustrates the necessity to use narrow components to fit the data. The overall fit, where subcomponents with $4 < b < 10 \text{ km s}^{-1}$ are used, is shown in the lower panel.

2712 (DI96) which are separated by $4h^{-1}$ Mpc, and it is very unlikely that a sheet of very small clouds would extend from one QSO to the other or that by chance material ejected by two independent QSOs would have the same velocity difference (Sargent & Steidel 1987). Finally, the system is not very highly ionized contrary to what is expected for gas close to the quasar (see typical associated systems in Petitjean et al. 1994).

Assuming that the system is made up of narrow components, we have fitted the C IV line profile. Since we do not resolve individual components, the fit cannot be unique. We assume therefore that individual components have Doppler parameters in a given range b_i - b_s . We evaluate the mean Doppler parameter by fitting the optical depths of both lines of the doublet (see Fig. 3 top panel) and find $b \sim 8 \text{ km s}^{-1}$. We have checked that the best fit is obtained with $b_i = 4$ and $b_s = 10 \text{ km s}^{-1}$. The global fit is given in Fig. 3 (lower panel). We conclude from this that the gas temperature is smaller than 10^5 K and probably smaller than $5 \times 10^4 \text{ K}$. Using the positions and Doppler parameters of the components derived from the fit, we then have fitted the Si IV, H I and N V wavelength ranges to derive column densities or upper limits.

The conditions are fairly homogeneous in the complex and typical column densities are $\log N \sim 13.2, 12.3, 13., 13.7$ and < 13 for H I, Si III, Si IV, C IV and N V respectively. The column density ratios are incompatible with ionization by a QSO-like spectrum. Indeed, from the large $N(\text{Si IV})/N(\text{C IV})$ ratio, the ionization parameter should be $U \sim 10^{-3}$ (see Bergeron & Stasińska 1986) whereas the large $N(\text{Si IV})/N(\text{Si III})$ ratio indicates $U \sim 0.1$. One way to solve the contradiction is to consider that the gas is photo-ionized by a stellar spectrum with no photons above 45 eV. This suggests that this system originates in a H II region (see also Viegas & Gruenwald 1991).

It should be then highly ionized with $\text{Si IV}/\text{Si} \sim \text{C IV}/\text{C} \sim 1$. In this case since 10^5 is a reasonable upper limit for $\text{H II}/\text{H I}$, the abundances should be larger than $0.1 Z_{\odot}$. Alternatively if the temperature is $T \sim 10^5$ K and the gas collisionally ionized, the ionization correction (see Arnaud & Rothenflug 1985) leads to carbon and silicon abundances of the order of 0.5 and 5 times the solar value respectively. Although we cannot firmly differentiate between both explanations, we can conclude that the gas is not photo-ionized by the QSO and has fairly high metallicity for such redshift.

3.2. The $z_{\text{abs}} \sim 2.133$ system

Although the C IV lines are particularly strong in this system, the line profiles are typical of a normal intervening system. In particular there is a strong H I absorption and the low-ionization species are spread over a velocity range much smaller than C IV. $\Delta V = 40, 40, 1200, 1200, 2200$ and 3000 km s^{-1} for O I, Fe II, Si II, C II, Si IV and C IV respectively.

The C IV profile is complex and heavily blended, so we concentrate our analysis on the O I, C II*, C II, Si II and Fe II lines (see Fig. 2). The fit of the lines has been performed assuming that the redshift and b values were the same for all species which is reasonable since the absorptions are expected to arise from the same phase. Since we see two well detached components in Fe II, we first tried to find a two-component model. This failed because the b values mostly constrained by Fe II were too large ($\sim 20 \text{ km s}^{-1}$) for the Si II $\lambda 1304$ fit to be acceptable. The obvious solution was that the system is made up of a larger number of narrower components. We find a good overall fit for O I, C II*, C II and Si II with four $b \sim 12 \text{ km s}^{-1}$ components. The Fe II profile imposes $b \sim 10 \text{ km s}^{-1}$. This can be understood if the lines arise in a medium with turbulent motions characterised by $b \sim 8 \text{ km s}^{-1}$ and $T \sim 50000 \text{ K}$. This values should be considered as upper limits.

We find that the total column densities are $\log N(\text{O I}, \text{C II}^*, \text{C II}, \text{Si II} \text{ and } \text{Fe II}) = 14.9, 14.0, 14.8, 14.6, 14.6$ respectively. If the C II column density can be considered as quite uncertain since it relies on a single strong line, this is not the case for other species which have at least one weak line. The H I Ly α line is redshifted in a part of the spectrum with moderate S/N ratio. However from the lack of damped wings (see Fig. 1 and DI96), we are confident that the total H I column density is smaller than $4 \times 10^{19} \text{ cm}^{-2}$.

We discuss the metallicities in the system compared to the logarithmic solar values: $-3.4, -3.2, -4.6$ and -4.5 for C, O, Fe and Si respectively. O I and H I being tied up by charge-exchange reaction, the $N(\text{O I})/N(\text{H I})$ column density ratio gives the oxygen abundance without need of any ionization correction. We thus conclude that the oxygen abundance is of the order of 0.03 solar.

Scaling photo-ionization models published in the literature (see Steidel 1990, Petitjean et al. 1994), we can derive relative abundances for other species. The above column densities indicate that the ionization parameter is smaller than 10^{-3} . For $\log N(\text{H I}) = 19.5$, and metallicities $Z = 0.01 Z_{\odot}$, the models give $\log N(\text{O I}, \text{C II}, \text{Si II} \text{ and } \text{Fe II}) \sim 14.5, 15.1, 14.1$ and 13.6 respectively. It can be seen that iron could be overabundant compared to oxygen by a factor of two to three.

The conclusion that the $[\text{Fe}/\text{O}]$ ratio is close to solar for an absolute abundance of the order of a hundredth of solar is intriguing. Indeed observations of metal deficient stars in the

halo of our galaxy indicate that for $[\text{Fe}/\text{H}] < -2$, $[\text{O}/\text{Fe}] > 0.5$ (Spite 1991), consistent with predictions of chemical evolution models (Matteucci & Padovani 1993).

The detection of the C II* $\lambda 1335$ line shows that the fine structure upper level of the C II ground-state is populated. If this is due to collisions and if it is assumed that the gas is completely ionized as suggested by the moderate H I column density ($\text{H I}/\text{H} < 1$), one can derive a value $n_e \sim 3 \text{ cm}^{-3}$ for the electronic density. We can combine the density and the ionization parameter derived from the ionization state of the gas to infer information about the ionizing flux. Using $F_{\nu} = F_o(\nu/\nu_o)^{-\alpha}$ with $\alpha = 0.5$ or 1.5 , we find that the flux at the Lyman limit should be of the order of $F_o = 5 \times 10^{-20}$ or $1.5 \times 10^{-19} \text{ erg cm}^{-2} \text{ s}^{-1} \text{ Hz}^{-1} \text{ sr}^{-1}$ respectively. This is much higher than the UV background from QSOs and early galaxies at this redshift (Miralda-Escudé & Ostriker 1990). Some additional source must contribute the ionization. If this is the quasar, we derive that the distance to the quasar should be larger than $0.3h^{-1} \text{ Mpc}$ ($q_o = 0.5$), using a typical luminosity of $F_o = 1.4 \times 10^{-28} \text{ erg cm}^{-2} \text{ s}^{-1} \text{ Hz}^{-1} \text{ sr}^{-1}$ (Sargent & Steidel 1991). This strongly suggests that the system is not associated with the QSO.

4. Conclusion

We have shown in the previous sections that the gas lying on the line of sight to Tol 1037-2704 is certainly not associated with the QSO since the physical state is notably different from that of BAL or associated systems (e.g. Wampler et al. 1995, Petitjean et al. 1994).

Most of the systems on the line of sight have column densities and ionization states typical of intervening systems with, when an estimate is possible, abundances of the order of 10^{-2} – $10^{-1} Z_{\odot}$. A detailed study of the O I, C II*, Si II and Fe II lines at $z_{\text{abs}} \sim 2.1393$ shows that the oxygen metallicity is of the order of $0.03 Z_{\odot}$ and $[\text{Fe}/\text{O}]$ is slightly larger than solar; the ionization parameter and electronic density are of the order of $U \sim 10^{-3}$ and $n_e \sim 3 \text{ cm}^{-3}$. The distance to the QSO is probably larger than $300h^{-1} \text{ kpc}$. The system at $z_{\text{abs}} \sim 2.08$ has a shallow and complex profile both on the line of sight to Tol 1037-2704 and Tol 1038-2712. The fact that the strengths of the two lines of the C IV and Si IV doublets are not in the oscillator strength ratios indicates that the complex is made up of narrow unresolved components. The temperature must be smaller than 10^5 K . The abundances are larger than $0.1 Z_{\odot}$. If the gas is photo-ionized, the ionizing spectrum must be stellar. Alternatively, the gas could be purely collisionally ionized. In this case however, silicon must be overabundant relative to carbon by a factor of ten.

These results strengthen the conclusion by Sargent & Steidel (1987) and DI96 that the material is part of an intervening supercluster. The latter authors have shown that the number of C IV systems toward Tol 1037-2704 and Tol 1038-2712 is much in excess of what is expected. As we confirm seven of their probable systems toward Tol 1037-2704, the number of systems with $w_r > 0.15 \text{ \AA}$ is equal to 16 to be compared with 2 expected from Poisson statistics. Considering coincidences of absorption redshifts in four lines of sight in the same field, they find also that there is a marginally significant correlation on comoving scales of $< 18 \text{ Mpc}$.

This altogether strongly suggests that we observe a supercluster which extends over $30 \times 80h^{-1} \text{ Mpc}^2$. Deep imaging

should be performed in this field to detect the luminous component of this large scale structure. *Acknowledgements.* We would

like to thank the referee, Chris Impey, who carefully reviewed our manuscript.

References

- Arnault M., Rothenflug R., 1985, A&AS 60, 425
 Bechtold J., Crotts A.P.S., Duncan C., Fang Y., 1994, ApJL 437, L83
 Bergeron J., Stasińska G., 1986, A&A 169, 1
 Bohuski T.J., Weedman D.W., 1979, ApJ 231, 653
 Cen R., Miralda-Escudé J., Ostriker J.P., Rauch M., 1994, ApJ 437, L9
 Cristiani S., Danziger I.J., Shaver P.A., 1987, MNRAS 227, 639
 Dinshaw N., Foltz C.B., Impey C.D., et al., 1995, Nature 373, 223
 Dinshaw N., Impey C.D., 1996, ApJ 458, 73 (DI96)
 Dinshaw N., Impey C.D., Foltz C.B., et al., 1994, ApJ 437, L87
 Evrard A.E., Charlot S., 1994, ApJL 424, L13
 Foltz C.B., Hewett P.C., Chaffee F.H., Hogan C.J., 1993, AJ 105, 22
 Francis P.J., Hewett P.C., 1993, AJ 105, 1633
 Heisler J., Hogan C.J., White S.D.M., 1989, ApJ 347, 52
 Hernquist L., Katz N., Weinberg D.H., Miralda-Escudé J., 1996, ApJ 457, L51
 Jakobsen P., Perryman M.A.C., 1992, ApJ 392, 432
 Jakobsen P., Perryman M.A.C., Ulrich M.H., et al., 1986, ApJ 303, L27
 Jenkins E.B., 1986, ApJ 304, 739
 Jing Y.P., Mo H.J., Börner G., Fang L.Z., 1995. In Mückel J.P., Gottlöber S., Müller V. (eds) Proc. Large Scale Structure in the Universe, World Scientific, Potsdam, p. 232
 Matteucci F., Padovani P., 1993, ApJ 419, 485
 Miralda-Escudé J., Ostriker J.P., 1990, ApJ 350, 1
 Morton D.C., 1991, ApJS 77, 119
 Morton D.C., York D.G., Jenkins E.B., 1988, ApJS 68, 449
 Mückel J., Petitjean P., Kates R.E., Riediger R., 1996, A&A 308, 17
 Ostriker J.P., 1993, ARAA 31, 689
 Petitjean P., 1995. In Danziger J., Walsh J. (eds) Proc. ESO Workshop, Science with VLT. Springer, Heidelberg, p. 339
 Petitjean P., Mückel J., Kates R.E., 1995, A&AL 295, L9
 Petitjean P., Rauch M., Carswell R.F., 1994, A&A 291, 29
 Rauch M., Haenelt M., 1996, MNRAS 275, L76
 Richstone D., Loeb A., Turner E.L., 1992, ApJ 393, 477
 Robertson J.G., 1987, MNRAS 227, 653
 Robertson J.G., Shaver P.A., 1983, MNRAS 204, 69P
 Sargent W.L.W., Steidel C.C., 1987, ApJ 322, 142
 Sargent W.L.W., Steidel C.C., 1991, ApJ 382, 433
 Sembach K.R., Savage B.D., 1992, ApJS 83, 147
 Shaver P.A., Robertson J.G., 1983, ApJL 268, L57
 Smette A., Robertson J.G., Shaver P.A., Reimers D., Wisotzki L., Köhler T., 1995, A&AS 113, 199
 Smette A., Surdej J., Shaver P.A., et al., 1992, ApJ 389, 39
 Spite M., 1991, In Barbuy B., Renzini A. (eds) Proc. IAU Symp., The Stellar populations of Galaxies, p. 123
 Steidel C.C., 1990, ApJS 74, 37
 Tripp T.M., Lu L., Savage B.D., 1996, ApJS 102, 239
 Ulrich M.H., Perryman M.A.C., 1986, MNRAS 220, 429
 Viegas S.M., Gruenwald R.B., 1991, ApJ 377, 39
 Wampler E.J., Chugai N.N., Petitjean P., 1995, ApJ 443, 586
 West M.J., 1994. In Durret F., Mazure A., Trân Thanh Vân J. (eds). Proc. of the XXIXth Rencontre de Moriond, Clusters of Galaxies. Frontières, Gif-sur-Yvette, p.23
 Weymann R.J., Carswell R.F., Smith M.G., 1981, ARA&A 19, 41
 Wolfe A.M., 1993, ApJ 402, 411